Communication

M35 Oxidation Induces A#40-like Structural and Dynamical Changes in A#42

Yilin Yan, Scott A. McCallum, and Chunyu Wang

J. Am. Chem. Soc., **2008**, 130 (16), 5394-5395 • DOI: 10.1021/ja711189c • Publication Date (Web): 01 April 2008

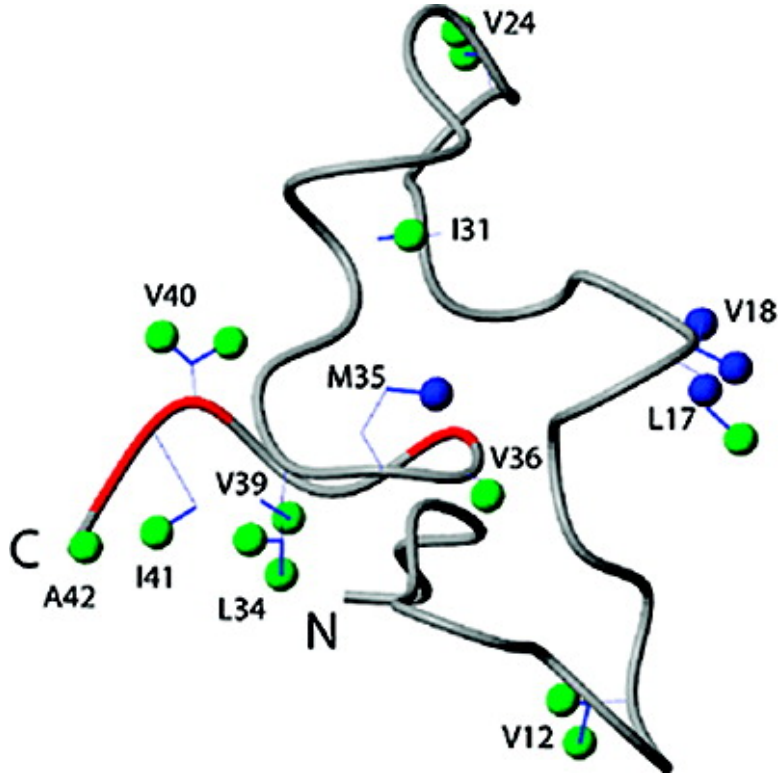

More About This Article

Additional resources and features associated with this article are available within the HTML version:

- Supporting Information
- Access to high resolution figures
- Links to articles and content related to this article
- Copyright permission to reproduce figures and/or text from this article

J|A|C|S
COMMUNICATIONS

Published on Web 04/01/2008

M35 Oxidation Induces Aβ40-like Structural and Dynamical Changes in Aβ42

Yilin Yan, Scott A. McCallum, and Chunyu Wang*
Biology Department, Center for Biotechnology and Interdisciplinary Studies, Rensselaer Polytechnic Institute, Troy, New York 12180
Received December 20, 2007; E-mail: wangc5@rpi.edu

Alzheimer's disease (AD) is the most common form of dementia whose pathology is characterized by intracellular neurofibrillary tangles and extracellular senile plaques.[1] Amyloid-β peptides (Aβ) are the major components of the senile plaque.[2] Aβ40 and Aβ42, composed of 40 and 42 amino acids, respectively, are the most abundant species of Aβ in the body. Despite 95% sequence identity between Aβ40 and Aβ42, their in vitro and in vivo properties are different.[3,4] Aβ42 aggregates much faster and is more toxic than Aβ40.[5,6] In addition, Aβ40 and Aβ42 have distinct pathways for oligomer formation.[7] NMR and molecular dynamics studies [8–12] have demonstrated structural and dynamical differences between Aβ40 and Aβ42 monomers, which contribute to their differences in aggregation and toxicity. The side chain of methionine 35 can be oxidized to sulfoxide and the oxidized form (Aβ^{ox}) comprises 10–50% of total brain Aβ in postmortem senile plaques.[13] Recent studies have shown delayed protofibril formation and reduced aggregation of Aβ42^{ox} compared to Aβ42^{red}.[14] Oligomer assembly of Aβ42 also becomes indistinguishable from that of Aβ40 after M35 oxidation.[7] However, it is not clear how M35 oxidation can cause such profound changes in Aβ42 aggregation.

In the current study, we investigated the structural and dynamical differences between Aβ42^{ox} and Aβ42^{red} monomers using solution NMR. Previously, we have shown that on the ps−ns time scale, the C-terminus of Aβ42 is more rigid than that of Aβ40 in both backbone and side chain while the methyl groups of V18 are more dynamic in Aβ42 than those in Aβ40.[9,10] Here, we show M35 oxidation causes a significant increase of the backbone mobility at the C-terminus and a significant decrease of the mobility of V18 methyl groups in Aβ42.

Uniformly ^{15}N and ^{15}N, ^{13}C labeled Aβ42 (rPeptide) monomers generated by HFIP treatment[15] was oxidized by H_2O_2.[14] The complete oxidation of Aβ42^{ox} has been confirmed by both NMR and MS. The backbone ^{15}N dynamics and side-chain methyl dynamics of Aβ42^{ox} monomer were measured and analyzed as described previously.[9,16]

Figure 1 shows the ^{1}H−^{15}N HSQCs of Aβ40 overlaid with that of Aβ42^{red} (A) and Aβ42^{ox} (B). Residues L34, M35, V36, G37, G38, and V39 of Aβ42 displayed chemical shift perturbation upon M35 oxidation. The changes toward the C-terminus, especially G37-V39 are not likely due to the extra oxygen since they remain in the same positions in Aβ40 before and after M35 oxidation.[12] Intriguingly, three residues G37, G38, and V39 of Aβ42^{ox} move closer to the positions where they are located in Aβ40^{red} in the HSQC. This strongly suggests that conformations of Aβ42 near the C-terminus, in particular between residues G37 and V39, have been altered to become more Aβ40-like by M35 oxidation. As shown by a previous CSI analysis,[12] Aβ40^{red} lacks β-sheet propensity at I31−V36 which is present in Aβ42^{red}. Oxidation of Aβ42 reduces the β-sheet propensity of

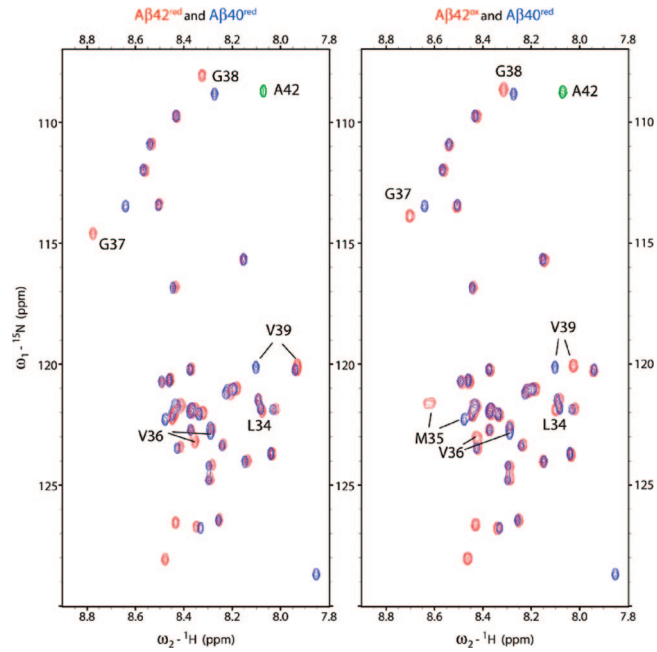

Figure 1. The overlaid ^{1}H−^{15}N HSQC spectra of Aβ42^{red} (red) and Aβ40^{red} (blue) (A) and overlaid HSQC spectra of Aβ42^{ox} (red) and Aβ40^{red} (blue) (B) at 273.3 K. Residues G37, G38, and V39 of Aβ42^{ox} display significant chemical shift perturbation and move toward where they are located in Aβ40^{red}, suggesting that conformation ensemble of Aβ42^{ox} has been changed to become more like that of Aβ40^{red}. A42 is in green owing to the spectra folding.

residues I31−V36, again suggesting Aβ42^{ox} experiences an Aβ40-like change in its conformational ensemble.

Previously, we have shown that without M35 oxidation the Aβ42 monomer has a more rigid C-terminus than Aβ40 monomer on the ps−ns time scale, which may promote the aggregation of Aβ42.[9,10] Here, we show that M35 oxidation significantly increases the C-terminal flexibility of Aβ42 therefore results in an Aβ40-like change in backbone ^{15}N dynamics. Aβ42^{ox} and Aβ42^{red} have similar backbone ^{15}N R_1 and R_2 values (Supporting Figure 1), indicating they have similar global motions. Excluding three C-terminal residues (V40-A42), the average NOE values are similar between Aβ42^{red} (0.47 ± 0.08) and Aβ42^{ox} (0.43 ± 0.09). In Aβ42^{red}, the NOE values of three C-terminal residues are 0.47 ± 0.01, 0.40 ± 0.03, and −0.27 ± 0.06 for V40, I41, and A42, respectively. The NOE values (0.14 ± 0.06, 0.21 ± 0.04, and −0.37 ± 0.06) of these three residues (V40, I41, and A42, respectively) in Aβ42^{ox} decrease dramatically (Figure 2A), demonstrating increased C-terminal flexibility on the ps−ns time scale. Consistent with trends in NOE values, $J(0.87\omega_H)$ values derived from reduced spectra density mapping (Figure 2B) are also lower for Aβ42^{red} C-terminal residues compared to those of Aβ42^{ox}. Residues 16, 23, 25, 26, 31, and 35 of Aβ42 also showed slightly increased

10.1021/ja711189c CCC: $40.75

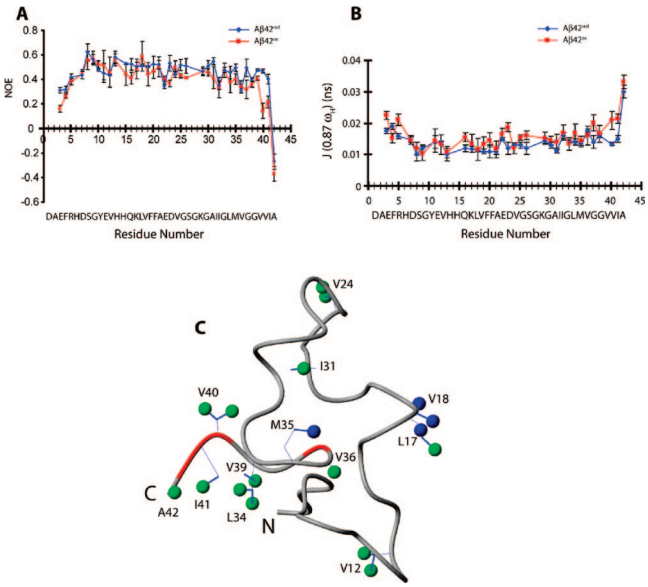

Figure 2. M35 oxidation alters the dynamics of Aβ42 on the ps−ns time scale. Backbone ^{15}N NOE (A) and $J(0.87\ \omega_H)$ values (B) indicate increased mobility of the C-terminus of Aβ42 upon M35 oxidation. (C) Backbone ^{15}N NOE difference ($NOE_{A\beta42}{}^{red} - NOE_{A\beta42}{}^{ox}$) and side-chain methyl groups $S^2{}_{A\beta42}{}^{ox}/S^2{}_{A\beta42}{}^{red}$ were mapped on to the ribbon diagram model of Aβ42 monomer from a replica-exchange MD simulation.[11] Backbone is shown in red if the NOE difference ($NOE_{A\beta42}{}^{red} - NOE_{A\beta42}{}^{ox}$) is bigger than 0.15, grey if $-0.15 < NOE_{A\beta42}{}^{red} - NOE_{A\beta42}{}^{ox} < 0.15$. Methyl groups are shown in blue if the ratio is bigger than 1.2, green if $0.83 < S^2{}_{A\beta42}{}^{red}/S^2{}_{A\beta42}{}^{ox} < 1.2$. The backbone residues of the C-terminus become more mobile and the methyl groups of M35, L17, and V18 become less mobile upon M35 oxidation.

$J(0.87\ \omega_H)$ values upon M35 oxidation, which was probably due to the reduced presence of the turn conformation between D23-K28 in Aβ42^{ox} suggested by Hou et al.[12]

Our recent methyl dynamics studies of Aβ40^{red} and Aβ42^{red} monomers demonstrated that Aβ42^{red} has a more rigid C-terminus than that of Aβ40^{red}.[9] We also observed that the methyl groups of a critical residue V18, located at the central hydrophobic cluster (CHC), is more rigid in Aβ40^{red} than those in Aβ42^{red}.[9] Here, we have investigated the effect of M35 oxidation on the methyl dynamics of Aβ42. As expected, the extra oxygen leads to the reduced motion of the side-chain methyl group of M35, with the order parameter values increasing from 0.073 ± 0.007 (Aβ42^{red}) to 0.17 ± 0.03 (Aβ42^{ox}). M35 oxidation increased side-chain mobility toward the C-terminus as indicated by the decrease of order parameter values by ~10% (Supporting Information, Table 2). More interestingly, the order parameters of methyl groups L17δ', V18γ, V18γ', I31γ in Aβ42^{ox} (0.51 ± 0.01, 0.68 ± 0.01, 0.82 ± 0.02, and 0.59 ± 0.01, respectively) increase significantly compared to those in Aβ42^{red} (0.33 ± 0.02, 0.45 ± 0.03, 0.51 ± 0.03, and 0.51 ± 0.01, respectively) (Figure 2B; Supporting Information, Tables 3 and 4). In contrast, the order parameter of V24γ' in Aβ42 decreases toward the corresponding value in Aβ40 upon M35 oxidation (Supporting Information, Table 4). Increased mobility of L34δ was observed, probably due to the increased polarity of the extra oxygen on M35 side chain. Overall, Aβ42 has experienced Aβ40-like changes in side-chain methyl dynamics upon M35 oxidation.

MD simulation and limited protease digest studies have suggested a turn involving G37-G38 in Aβ42 which is absent in Aβ40. This is consistent with chemical shift changes in backbone amides in Figure 1.[11,17–19] The C-terminal dynamics difference between Aβ40^{red} and Aβ42^{red} monomers is likely caused by the presence of the transient G37-G38 turn. The turn in Aβ42^{red} monomer significantly increases the hydrophobic contact between L34-V36 and V39-A42 located at the C-terminus as compared to Aβ40^{red}.[18] This could explain the reduced C-terminal flexibility of Aβ42^{red} monomer as shown by our previous backbone and side-chain dynamics data.[9,10] We also speculate that the G37-G38 turn in Aβ42^{red} may prevent the hydrophobic intramolecular interaction between CHC and residues A30-M35, which may contribute to the increased mobility of V18 side-chain in Aβ42^{red}.[9] After M35 is oxidized, the sulfoxide ($\epsilon CH_3S{=}O$) group of Aβ42^{ox} likely hinders the transient G37-G38 turn conformation. Thus, the C-terminus of Aβ42^{ox} becomes more mobile. The absence of the G37-G38 turn may lead to intramolecular interaction between Aβ A30-M35 and CHC, causing reduced motion of L17, V18, and I31. The presence or absence of the G37-G38 turn likely affects backbone dynamics more than side-chain dynamics, while the presence or absence of the hydrophobic interaction involving CHC should affect side-chain dynamics more than backbone dynamics. This explains why major changes in backbone dynamics occur only in the C-terminus while major changes in side-chain dynamics occur mostly in CHC. A weakness in our hypothesis is that A30-M35, the region proposed to interact with CHC in Aβ42^{ox}, does not experience a significant restriction in methyl dynamics upon M35 oxidation. It may be speculated that A30-M35 is involved in other hydrophobic interactions in Aβ42^{red}.

In summary, we utilized NMR to investigate the backbone and side-chain dynamics of Aβ42^{ox} monomer on the ps−ns time scale. We revealed that M35 oxidation of Aβ42 induces Aβ40-like structural and dynamical changes probably by preventing the G37-G38 turn conformation, which contributes to its reduced aggregation and toxicity.

Supporting Information Available: Detailed description of NMR experiments and analysis, tables of relaxation rates and figures of J-coupling, RDC and ^{15}N R_1 and R_2 rates of Aβ42^{ox} and Aβ42^{red}. This material is available free of charge via the Internet at http://pubs.acs.org.

References

(1) Selkoe, D. *J. Physiol. Rev.* **2001**, *81*, 741–66.
(2) Roher, A. E.; Lowenson, J. D.; Clarke, S.; Woods, A. S.; Cotter, R. J.; Gowing, E.; Ball, M. *J. Proc. Natl. Acad. Sci. U.S.A.* **1993**, *90*, 10836–40.
(3) Jarrett, J. T.; Berger, E. P.; Lansbury, P. T., Jr *Ann. N.Y. Acad. Sci.* **1993**, *695*, 144–8.
(4) Selkoe, D. J. *Neuron* **1991**, *6*, 487–98.
(5) Chen, Y. R.; Glabe, C. G. *J. Biol. Chem.* **2006**, *281*, 24414–22.
(6) Zhang, Y.; McLaughlin, R.; Goodyer, C.; LeBlanc, A. *J. Cell Biol.* **2002**, *156*, 519–29.
(7) Bitan, G.; Tarus, B.; Vollers, S. S.; Lashuel, H. A.; Condron, M. M.; Straub, J. E.; Teplow, D. B. *J. Am. Chem. Soc.* **2003**, *125*, 15359–65.
(8) Riek, R.; Guntert, P.; Dobeli, H.; Wipf, B.; Wuthrich, K. *Eur. J. Biochem.* **2001**, *268*, 5930–6.
(9) Yan, Y.; Liu, J.; McCallum, S. A.; Yang, D.; Wang, C. *Biochem. Biophys. Res. Commun.* **2007**, *362*, 410–4.
(10) Yan, Y.; Wang, C. *J. Mol. Biol.* **2006**, *364*, 853–62.
(11) Sgourakis, N. G.; Yan, Y.; McCallum, S. A.; Wang, C.; Garcia, A. E. *J. Mol. Biol.* **2007**, *368*, 1448–57.
(12) Hou, L.; Shao, H.; Zhang, Y.; Li, H.; Menon, N. K.; Neuhaus, E. B.; Brewer, J. M.; Byeon, I. J.; Ray, D. G.; Vitek, M. P.; Iwashita, T.; Makula, R. A.; Przybyla, A. B.; Zagorski, M. G. *J. Am. Chem. Soc.* **2004**, *126*, 1992–2005.
(13) Kuo, Y. M.; Kokjohn, T. A.; Beach, T. G.; Sue, L. I.; Brune, D.; Lopez, J. C.; Kalback, W. M.; Abramowski, D.; Sturchler-Pierrat, C.; Staufenbiel, M.; Roher, A. E. *J. Biol. Chem.* **2001**, *276*, 12991–8.
(14) Hou, L.; Kang, I.; Marchant, R. E.; Zagorski, M. G. *J. Biol. Chem.* **2002**, *277*, 40173–6.
(15) Lim, K. H.; Kim, Y. K.; Chang, Y. T. *Biochemistry* **2007**, *46*, 13523–32.
(16) Zhang, X.; Sui, X.; Yang, D. *J. Am. Chem. Soc.* **2006**, *128*, 5073–81.
(17) Urbanc, B.; Cruz, L.; Yun, S.; Buldyrev, S. V.; Bitan, G.; Teplow, D. B.; Stanley, H. E. *Proc. Natl. Acad. Sci. U.S.A.* **2004**, *101*, 17345–50.
(18) Yun, S.; Urbanc, B.; Cruz, L.; Bitan, G.; Teplow, D. B.; Stanley, H. E. *Biophys. J.* **2007**, *92*, 4064–77.
(19) Lazo, N. D.; Grant, M. A.; Condron, M. C.; Rigby, A. C.; Teplow, D. B. *Protein Sci.* **2005**, *14*, 1581–96.

JA711189C